DCS Tx filters using AlN resonators with Iridium electrodes

M. Clement, E. Iborra, J. Olivares
GMME Universidad Politécnica de Madrid
Madrid, Spain
mclement@etsit.upm.es

N. Rimmer
Aviza Technology Inc.
Newport, South Wales, UK

S. Giraud, S. Bila
XLIM UMR 6172 - Université de Limoges/CNRS
Limoges, France

A. Reinhardt
CEA, Leti, Minatec,
Grenoble, France

***Abstract*— In this paper we present the design methodology, fabrication technology and characterization of bulk acoustic wave (BAW) filters for the DCS Tx-band at 1.75GHz. The filters are fabricated with solidly mounted AlN-based resonators (SMR) using iridium metallic electrodes, in an attempt to increase the effective electromechanical coupling factor of the BAW devices and achieve the bandwidth requirements of DCS filters. The design and optimization of the filters is performed with a simulation tool that uses a circuital model to compute the filter frequency response. Tx filters with balanced inputs and outputs and different topologies are designed and fabricated. The experimental filter response is compared with the simulations to determine the suitability of each design. Bandwidth DCS requirements are fulfilled by using Ir/AlN/Ir stacks.**

I. INTRODUCTION

Band-pass filters made with bulk acoustic wave (BAW) resonators based on aluminum nitride (AlN) are currently used in consumer products for mobile communication systems such as Digital Cellular System (DCS) and Wideband Code Division Multiple Access (WCDMA) [1-4].

Digital Cellular System 1800 (DCS 1800) is a global system for mobile communications-based PCS networks. DCS has a transmitter or uplink band (Tx-band) between 1710 MHz and 1785 MHz and a receiver or downlink band (Rx-band) between 1805 MHz and 1880 MHz, their relative bandwidths being of 4.3% and 4%, respectively. These relative bandwidths are significantly high, so special care is required for the design and fabrication technology of such DCS filters, especially for the Tx-band, which has the most demanding specifications (see Fig. 1).

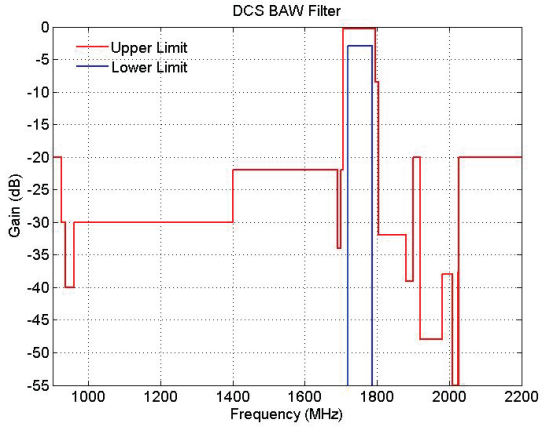

Figure 1. DCS filter specifications.

BAW pass-band filters are obtained by combining two types of BAW resonators: a low-frequency resonator (shunt or parallel resonator), whose resonant frequency is slightly lower than the low-band edge of the filter, and a high-frequency resonator (series resonator), whose anti-resonant frequency is slightly higher than the high-frequency edge of the filter. To maximize the bandwidth of the filter and minimize its in-band ripple, the resonant frequency of the high-frequency resonator and the anti-resonant frequency of the low-frequency resonator should coincide. Additionally, the bandwidths of BAW filters are directly related to the effective coupling factors of the BAW resonators (k_{eff}^2), which in turn depend on the piezoelectric activity of their active layers. The large relative bandwidth of the Tx filters in DCS systems (4.3%) requires BAW resonators with an effective coupling factor (k_{eff}^2) exceeding 7%. To achieve these specifications with AlN piezoelectric films, both a precise design of the BAW resonator structure and AlN films exhibiting a piezoelectric

978-1-4244-3510-4/09/$25.00 ©2009 IEEE

activity as intense as possible are required. Regarding the quality factors (Q) of the resonators in the DCS filters, as the separation between the downlink and uplink bands is high (around 20 MHz), the exigencies of this factor are not too high.

The acoustic isolation of a BAW resonator is commonly achieved by placing an acoustic reflector (Bragg mirror), composed of a set of λ/4 layers alternating low and high acoustic impedance, between the resonator and substrate. The resulting structure is called solidly mounted resonator (SMR). To increase the effective coupling factor of an SMR, a careful design of the whole structure (the Bragg mirror and the piezoelectric capacitor of the AlN piezoelectric layer between the two metallic electrodes) is required. Firstly, the Bragg acoustic reflectors should be composed of materials with low acoustic losses and exhibit acoustic transmission coefficients below -35 dB at the operating frequency, to achieve high quality and coupling factors. Regarding the piezoelectric stack, many parameters have to be considered apart from the optimized piezoelectric response of the AlN layer. The nature and crystalline structure of the bottom electrode are essential to achieve AlN films with a high piezoelectric activity; Al, Pt, Mo, W, or Ir are the most indicated metals to guarantee the growth of AlN films with the required crystalline and piezoelectric characteristics. Besides, the metal electrodes take also part in the propagation of the acoustic waves: high acoustic impedance metals exhibiting low acoustic losses are preferred, as they provide a more efficient confinement of the acoustic energy in the AlN layer. On the other hand, the ratio between the thicknesses of the electrodes and of the AlN layers sets the maximum value of the effective coupling factor that can be achieved for a given piezoelectric coefficient (d_{33}) [5, 6]. Finally, the choice of the loading material for the parallel resonators in the filter also influence notably the value of k_{eff}^2; larger values are obtained when loading the resonators with the same material as that of the top electrode, instead of using lighter materials such as SiO_2 [7, 8].

The demanding specifications of DCS filters cannot be achieved in SMR configurations using conventional molybdenum electrodes, for which the maximum achievable effective coupling factors are below 6.3% [9]. Iridium is a high-density noble metal that combines a high acoustic impedance [10], a low electric resistivity, and a specific crystal structure that promotes the growth of AlN films of excellent piezoelectric activity [11]. It can me considered, thus, as a solid candidate as an electrode in the fabrication of the exigent DCS filters. In fact, in previous works we have achieved k_{eff}^2 values greater than 7% in SMR devices with Ir electrodes.

In this paper we present the design, fabrication technology and characterization of DCS Tx-filters composed of SMR devices made of AlN piezoelectric stacks with iridium electrodes.

II. TECHNOLOGY

SMRs were fabricated by depositing Ir/AlN/Ir stacks on top of all-insulating Bragg mirrors formed by alternating low and high acoustic impedance layers of SiOC (Z_a=3.6×10^6 N·s·m^{-3}) and Si_3N_4 (Z_a=25.7×10^6 N·s·m^{-3}), similar to those described in a previous work [12].

Figure 2 shows a diagram of the structure of the whole device. Seed layers of Mo/Ti were sputtered on the last SiOC reflector layer to improve the adhesion and crystal quality of the Ir bottom electrode. Ir slugs (99.98% pure) were then electron-beam evaporated at a base pressure below 1×10^{-6} Torr to form bottom electrodes of different thicknesses ranging from 80 nm to 130 nm. The bottom electrode was patterned through a Mo mask by reactive ion etching (RIE), first in pure Ar^+ to remove the Ir layer, and then in SF_6 to remove the Mo/Ti seed layer. AlN piezoelectric films were then reactively sputtered with a pulsed DC source in a Sigma fxP cluster tool from Aviza Technology.

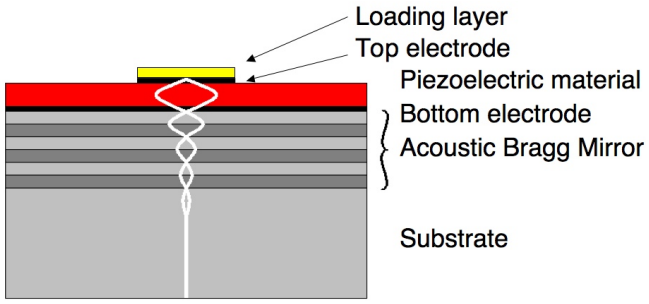

Figure 2. Solidly mounted resonator (SMR) schematics. The white lines are a representation of the distribution of the acosutic wave at the resonant frequency.

Before AlN deposition, a soft-etch in an Ar discharge was performed for 15 s to prepare the Ir bottom electrode [11]. After degassing the wafers to a temperature close to that of AlN deposition, AlN films were sputtered in a 1:5 Ar/N_2 mixture at a total pressure of 5 mTorr, a pulsed DC power of 10 kW, and a substrate temperature of 400ºC. An RF bias was applied to the substrates order to obtain stress-free AlN films (with a maximum deviation of 50 MPa). These conditions provided deposition rates of 100 nm/min with in-wafer thickness homogeneity of 0.3% 1σ. Ir top electrodes were then evaporated (to a thickness greater than that required to obtain the lower resonant frequency) and patterned by Ar^+ ion etching through a Mo mask; this was subsequently removed in a wet solution compatible with the Bragg mirror materials. A second Mo mask was used to open the vias through the AlN film in a KOH solution at 50ºC until the Ir bottom electrode was reached. Finally, the contact pads in the top and bottom electrodes were re-grown with a 1 µm-thick Al layer to reduce the contact resistance during probing or bonding.

Different Ir-based test SMRs and filters in the DCS band were fabricated following this technology. The tuning of the series and parallel resonators of the filters was achieved by partially etching their Ir top electrode in two steps. First, the top electrode in the whole wafer was progressively etched until the resonant frequency (f_r) of the parallel resonators was reached. The parallel resonators were then masked to adjust the resonant frequency of the series resonators. This was achieved by a further etching of their top electrode, until a resonant frequency identical to the anti-resonant frequency (f_a) of the parallel resonators was obtained. This process yielded two families of resonators (series and parallel) that only

differentiate in the thickness of the top electrode. This minimizes the differences between the effective coupling factor k_{eff}^2 of series and parallel resonators.

Figure 3 shows the shift of the resonant frequency f_r of a typical resonator with the thickness of the top electrode during the trimming process. Etching time is shown in the top axis. The variation of k_{eff}^2 is shown as well. The coupling was derived from the following equation:

$$k_{eff}^2 = \frac{\pi^2}{4}\frac{f_a - f_r}{f_a} \quad (1)$$

The thickness range depicted is that needed to obtain the resonant frequencies of the series and parallel resonators. We observe that k_{eff}^2 values are very close (and even larger) to 7% and vary slightly between loaded and non-loaded resonators. Additionally, the quality factor Q, which is around 500 for this particular test device, does not change significantly when deloading.

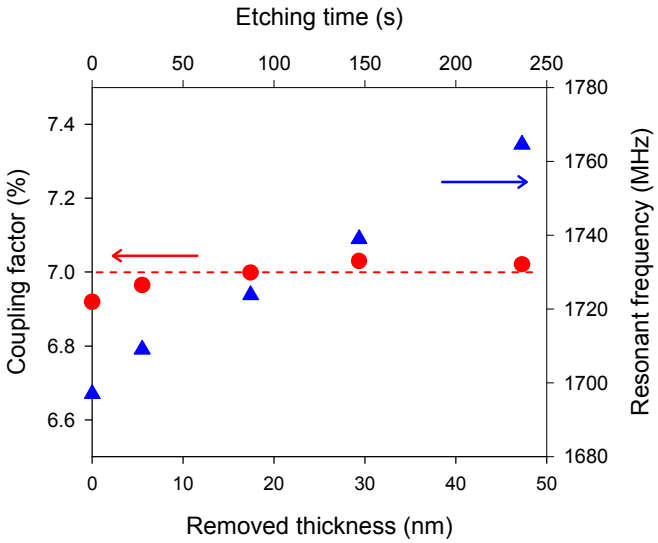

Figure 3. Variation of k_{eff}^2 (●) and f_r (▲) with the top electrode thickness during trimming process. Etching time is shown in the top axis.

III. BAW FILTER SYNTHESIS

BAW filters have been designed using a certain number of resonators with different frequencies and geometries. The number of resonators used to design a BAW filter varies between 6 and 16. To carry out this design it is necessary to use models of the response of the resonators that allow calculating the response of the filter. The typical electrical impedance of a BAW resonator is presented in Fig. 4 as a function of the frequency.

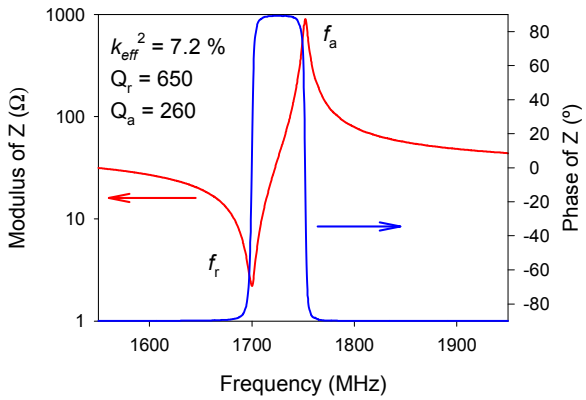

Figure 4. Modulus and phase of the electrical impedance of a typical BAW resonator.

This response can be easily fitted with several models, which can be used as a part of a design tool. The two models more commonly used are Mason's physical model, which simulates the electrical spectrum from the material constants and geometry of the resonator, and the Modified Butterworth Van Dyke (MBVD) behavioral circuital model, which is depicted in Fig. 5.

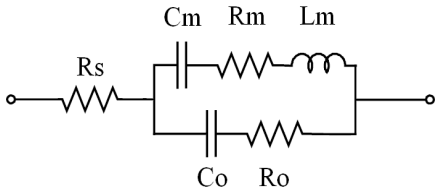

Figure 5. MBVD model of a BAW resonator.

L_m C_m and R_m represent the motional behavior of piezoelectric resonators; R_m accounts for the mechanical losses. R_0 and C_0 are the electrostatic resistance and capacitance of the resonator, respectively, given by the dielectric permittivity, the thickness of the piezoelectric layer and the area of the resonator. Finally, R_S represents the electrical losses owing to the electrodes.

R_m, R_S and R_0 are proportional to the quality factors Q_r and Q_a calculated at the resonant and anti-resonant frequencies, respectively. For the MBVD model,

$$f_r = \frac{1}{2\pi\sqrt{L_m C_m}} \quad (2)$$

$$f_a = f_r\sqrt{1 + \frac{C_m}{C_0}} \quad (3)$$

When design is the targeted application, the circuital model is more convenient than the physical model, as the calculations are faster and as the model can be easily included in circuit software. As we have already mentioned, BAW filters are usually designed using two types of resonators, namely, the series and the parallel resonators. Since the resonators are fabricated on the same wafer, the thickness of

the piezoelectric layer is fixed. However, as we explained in the previous section, a pass-band response can be achieved by adjusting the thicknesses of their top electrodes

Two main topologies can be used to make BAW filters:

A. Ladder Filter

In the ladder topology (Fig. 6), the parallel resonators are loaded in order to match their anti-resonant frequency with the resonant frequency of the series resonators. In order to obtain a pass-band characteristic (matching the inner electrical impedance), the areas of the resonators are optimized. The ladder structure allows to achieve a high selectivity, but yields a low out-of-band rejection. Some of these basic structures could be cascaded to obtain a better out-of-band rejection, but to the cost of generating higher insertion losses.

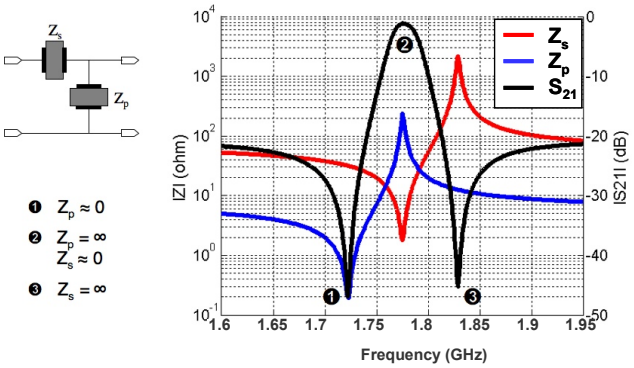

Figure 6. Ladder topology.

B. Lattice Filter

In the lattice topology (Fig. 7), parallel resonators are loaded in order to match their impedance level to that of series resonators. This lattice structure allows to obtain a larger out-of-band rejection, although its selectivity is low.

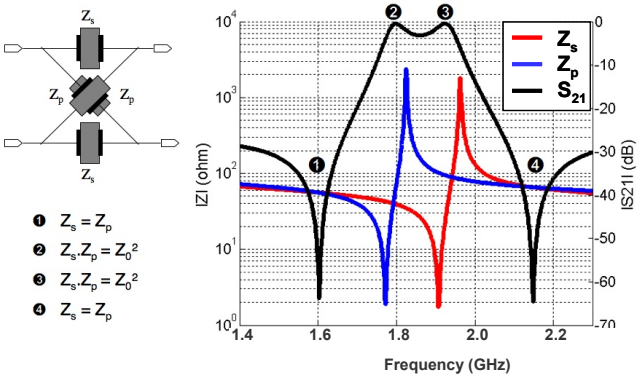

Figure 7. Lattice topology.

IV. Filters Design

A. Filter Design Methodology

The methodology of the design of the filters consists of 4 steps, as shown Fig. 8:

1. Introduction of technological data extracted from measurements of single BAW resonators (f_r, f_a, k_{eff}^2, Q_r, and Q_a).
2. Filter synthesis based on optimization of a lumped element model.
3. Drawing of the layout from the synthesized filter.
4. Verification analysis (co-simulation), including electromagnetic modeling of the layout.

Following this methodology, technological data are used for updating BAW resonator models in the filter synthesis module, regarding electrical specifications.

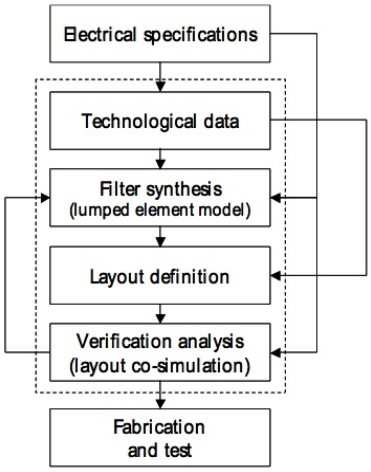

Figure 8. BAW filter design methodology.

The filter synthesis sets the BAW filter architecture and the characteristics of each resonator with respect to the electrical specifications. The specifications consist in a pattern giving the maximum/minimum transmission values in the pass-band and stop-band regions. The main output is the area of each resonator.

The layout of the filter can be drawn knowing the area of each resonator and the filter architecture; then, verification analysis is performed via a co-simulation including electromagnetic modeling, which allows characterizing both the losses owing to interconnections and the eventual coupling between the resonators. If the verification analysis does not meet the required specifications, the layout can be modified to reduce interconnection losses or coupling between the resonators. If this is not sufficient, the filter synthesis step must be repeated, increasing margins in the transmission pattern.

The core of the design methodology is the synthesis procedure based on the optimization of the MBVD model.

B. Filter synthesis and optimization

In order to synthesize and optimize BAW filters, we have developed a home-made simulation tool. This software, using the Matlab platform, is based on the MBVD model. It enables to compute complex frequency responses, such as those

shown by our filters, by considering the electrical impedances of the BAW resonators for different topologies. The proposed filter synthesis procedure is described in Fig. 9.

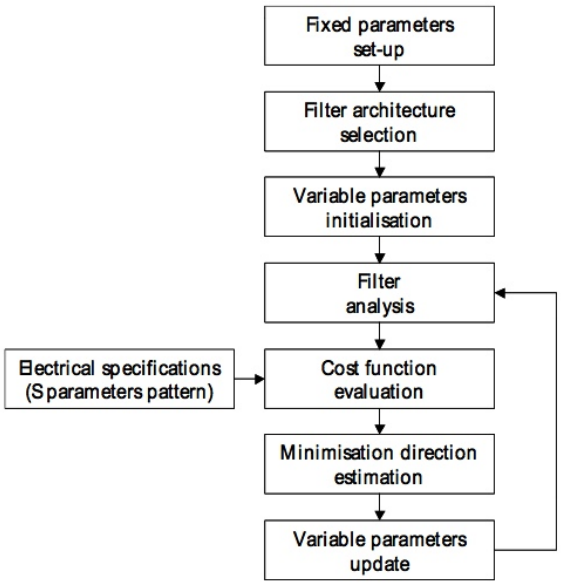

Figure 9. Filter synthesis procedure.

The synthesis starts with the initialization of the MBVD parameters of the resonators and the selection of the filter architecture.

The variable resonator parameters are optimized by minimizing a cost function which depends on the specifications of the *S* parameters. The synthesized response is optimized by comparing it with a given frequency pattern. This leads to a cost-function calculation. Then, by minimizing this function, we can extract the optimized value of each MBVD element that best fulfills the frequency response constraints.

C. *DCS Filter synthesis*

We performed the synthesis and the optimization of band-pass filters at 1.75GHz (Tx DCS frequencies) for different topologies. For each case, synthesis was performed with differential structures and a 100 Ω differential input and output impedance.

Figures 10 and 11 show the measurements and simulations of two filters with different topologies. The configuration of each topology is shown on the left side of the figures, and the actual layout in the inset on the right side. Note that the blue areas correspond to the loaded (parallel) resonators. The filter in Fig.10 has a series-parallel-series ladder configuration, whereas that in Fig. 11 has a two-stage lattice topology. It is important to note that the area of the ladder filter is significantly larger than that of the lattice filter. Therefore, the latter is more suitable for miniaturization. However, with lattice topologies only filters with differential input and output can be designed.

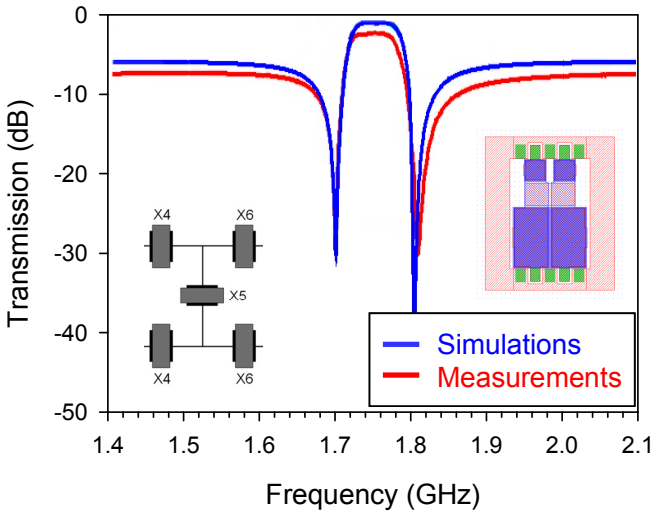

Figure 10. Series-parallel-series stage ladder filter.

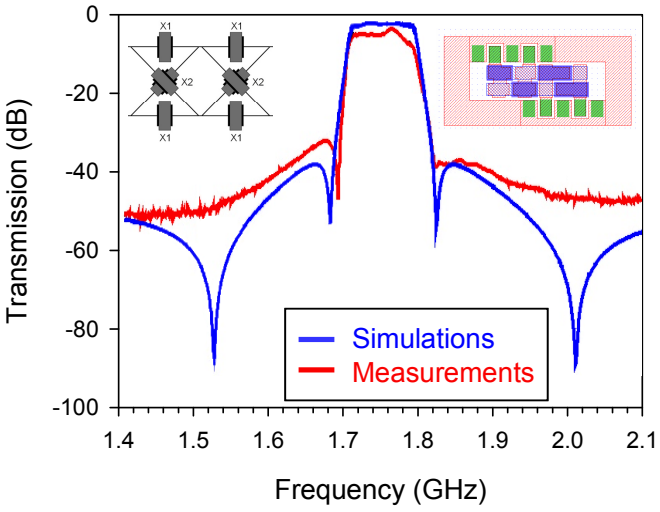

Figure 11. Two- stage lattice filter.

Both figures demonstrate that the agreement between simulated and measured responses is quite good. However, it is important to mention that the electrical losses (series resistance, contact resistance) of iridium were not taken into account in this first approach, so a better agreement is expected in further simulations. We observe that although the ladder filters fulfill the DCS specification regarding the insertion losses (<3 dB) and the filter width, their out-of-band rejection is excessive, as predicted by simulations. On the other hand, lattice filters exhibit a suitable out-of-band rejection (< 20 db), although their insertion losses in practical devices are still too large.

V. CONCLUSIONS

In this work, we have demonstrated how to build Tx filters with DCS specifications, whose main innovation is the use of iridium layers as bottom and top resonator electrodes. This provides the effective electromechanical coupling factor

required for DCS Tx filters. We also present a design methodology for BAW filters based on a local optimization method. Our filter synthesis software based on the MBVD model is a powerful tool that permits to optimize the area of each resonator with technological data extracted from measurements. A good agreement between the simulated and the measured filter response is obtained, which validates our approach.

ACKNOWLEDGMENT

The authors acknowledge financial support from the European Commission in the FP6 IST 2004-027003 MOBILIS project and all MOBILIS partners for their contributions.

REFERENCES

[1] R. Aigner, "Bringing BAW Technology into Volume Production: The Ten Commandments and the Seven Deadly Sins" Proc 3rd Int Symposium on Acoustic Wave Devices for Future Mobile Communication Systems, Chiba, Japan, Mar.(2007). pp.85-91

[2] E. Schmidhammer, H. Heinze, M. Schmiedgen, M. Mayer, and A. Link, "High Volume Production of a Fully Matched 5050 PCS-CDMA-BAW Duplexer" 2006 IEEE Ultrason. Symp. Proc., (2006) pp. 329-332.

[3] Jae Y. Park, Hee C. Lee, Kyeong H. Lee, Young J. Ko, and Jong U. Bu, "Silicon Bulk Micromachined FBAR Filters for W-CDMA Applications", 33rd European Microwave Conference Proc., (2003) pp. 907-910

[4] A. Volatier, E. Defaÿ, A. N'hari, J. F. Carpentier, P. Ancey, B. Dubus, "6H-5 Design, Elaboration and Characterization of Coupled Resonator Filters for WCDMA Applications", 2006 IEEE Ultrason. Symp. Proc., (2006) pp. 829-832.

[5] M Lakin, J. Belsick, J.F.McDonald, K.T. McCarron, "Improved bulk wave resonator coupling coefficient for wide bandwidth filters", 2001 IEEE Ultrasonics Symposium Proc. Vol. 1, (2001) pp 827- 831.

[6] M. Clement, J. Olivares, E. Iborra, S. González-Castilla, J. Sangrador, N. Rimmer, A. Rastogi, B. Ivira, A. Reinhardt, "Aluminum Nitride Solidly Mounted BAW resonators with Iridium electrodes", EFTF 2008 Proc., (2008) 0159.

[7] E. Iborra, M. Clement, J. Olivares, S. Gonzalez-Castilla, J. Sangrador, N. Rimmer, A. Rastogi, B. Ivira, and A. Reinhardt, "BAW resonators based on AlN with Ir electrodes for digital wireless transmissions." 2008 IEEE Ultrason. Symp. Proc., (2008) pp. 2189-2192.

[8] B. Ivira, P. Benech, R. Fillit, F. Ndagijimana, P. Ancey, and G. Parat, "Self-Heating Study of Bulk Acoustic Wave Resonators Under High RF Power" IEEE Trans. Ultrason. Ferr. Freq. Control, 55, (2008). pp. 139-147.

[9] A. Reinhardt, F. de Crécy, M. Aïd, S. Giraud, S. Bila, and E. Iborra, "Design of Computer Experiments: A powerful tool for the numerical design of BAW filters" 2008 IEEE Ultrason. Symp. Proc., (2008) pp. 2185-2188.

[10] A. Devos, E. Iborra, J. Olivares, M. Clement, A. Rastogi, and N. Rimmer, "Picosecond Ultrasonics as a Helpful Technique for Introducing a New Electrode Material in BAW Technology: The Iridium Case" 2007 IEEE Ultrason. Symp. Proc., (2007) pp. 1433-1436.

[11] M. Clement, J. Olivares, E. Iborra, S. González-Castilla, N. Rimmer, and A. Rastogi, "AlN films sputtered on iridium electrodes for bulk acoustic wave resonators", Thin Solid Films, 2009 in press.

[12] A. Reinhardt, N. Buffet, A.Shirakawa, J. B. David, G. Parat, M. Aid, S. Joblot, P. Ancey, "Simulation of BAW resonators frequency adjustment", Proc. 2007 IEEE Ultrasonics Symposium, (2007) pp. 1444-1447.